PERGAMON

Chaos, Solitons and Fractals 12 (2001) 1917–1927

CHAOS
SOLITONS & FRACTALS

www.elsevier.nl/locate/chaos

Analysis of period-doubling and chaos of a non-symmetric oscillator with piecewise-linearity

Q. Cao [a], L. Xu [a], K. Djidjeli [b,*], W.G. Price [b], E.H. Twizell [c]

[a] *Department of Mathematics and Physics, Shandong University of Technology, Jinan 250061, People's Republic of China*
[b] *Department of Ship Science, University of Southampton, Southampton SO17 1BJ, UK*
[c] *Department of Mathematical Sciences, Brunel University, Uxbridge, Middlesex UB8 3PH, UK*

Accepted 28 June 2000

Abstract

This paper presents an analysis of the dynamical behaviour of a non-symmetric oscillator with piecewise-linearity. The Chen–Langford (C–L) method is used to obtain the averaged system of the oscillator. Using this method, the local bifurcation and the stability of the steady-state solutions are studied. A Runge–Kutta method, Poincaré map and the largest Lyapunov's exponent are used to detect the complex dynamical phenomena of the system. It is found that the system with piecewise-linearity exhibits periodic oscillations, period-doubling, period-3 solution and then chaos. When chaos is found, it is detected by examining the phase plane, bifurcation diagram and the largest Lyapunov's exponent. The results obtained in this paper show that the vibration system with piecewise-linearity do exhibit quite similar dynamical behaviour to the discrete system given by the logistic map.

1. Introduction

The dynamical behaviour of non-linear systems have been well investigated since Lorenz found the strange attractor in 1963 (see for example [1,2]). The study of non-linear dynamical systems is still an interesting field of research, and particularly the study of chaos in non-linear systems (see for instance [3,4]). Methods used to detect chaos have been developed for non-linear systems; period-doubling and period-3 solution are familiar routes to chaos. Komatsu et al. [5], for example, studied the non-linear behaviour of the Duffing system, and found period-doubling bifurcation and chaos, and Li and York theorem [6] showed that period-3 implies chaos. The theorem of Li and York is often used to predict the chaotic motion of a non-linear system, based on the Sharkovsky sequence [7] (the details of the proof can be found in [8]).

In recent years, much attention has been paid to the study of a system with piecewise-linearity (see for instance, [9,10]). This oscillator is a typical non-linear system and is widely used in engineering systems (for example, in rotor systems [11], relaxation oscillator systems [12], hysteresitic networks [13] and circuit systems [14,15]). Studies show that systems with piecewise-linearity can exhibit complex behaviour (see for instance, Freire et al. [9,16], who studied the transition of the system from steady state to limit cycle).

The aim of this paper is to investigate the dynamical behaviour of a non-symmetric oscillator with piecewise-linearity. The C–L method is used to obtain the averaged system of the oscillator for the study of local bifurcation and the stability of the steady-state solutions. A Runge–Kutta method, Poincaré map and

* Corresponding author.
E-mail address: gamil@ship.soton.ac.uk (K. Djidjeli).

0960-0779/01/$ - see front matter
PII: S0960-0779(00)00155-7

Lyapunov's exponent are used to detect the chaotic motion of the system. It is found that a system with piecewise-linearity exhibits rich dynamical phenomena such as periodic oscillation, bifurcation and chaotic motion. The chaotic motion in the system can be predicted from the period-doubling, period-3 solution and the largest Lyapunov's exponent.

2. Model of the vibration system with a piecewise-linearity

Consider a vibration system with a piecewise-linearity shown in Fig. 1.

Fig. 1 is a model of a vibrating sieve with a distance d between the mass m and the spring k_1. When the system vibrates, the contact/separation of the spring and the mass form a non-symmetric non-linear vibration system with piecewise-linearity. The parameters k_1, k_2, f_1, f_2 and $d_0 - d$ in Fig. 1 refer to stiffness of the springs, dampings and the distance of compression under the static state, respectively.

The equation of motion for this system can be written in the form

$$m\ddot{x} + F(x,\dot{x}) + Q(x) = F_0 \sin(\omega t), \tag{1}$$

where

$$F(x,\dot{x}) = \begin{cases} (f_1 + f_2)\dot{x}, & x > -d, \\ f_1\dot{x}, & x \leqslant -d, \end{cases} \qquad Q(x) = \begin{cases} (k_1 + k_2)x, & x > -d, \\ k_1 x + k_1(d_0 - d), & x \leqslant -d. \end{cases} \tag{2}$$

3. Chen–Langford (C–L) method and local bifurcation

In this section, the C–L method is used to obtain the averaged equation of the system. Using this averaged system, the local bifurcation, the stability of the steady-state solutions and the phase portrait of the system are discussed.

3.1. Averaged system

Eq. (1) will be rewritten in the form

$$\ddot{y} + y = f(y,\dot{y}) + F\sin(\Omega t), \tag{3}$$

where

$$f(y,\dot{y}) = \begin{cases} -Ky - 2(A+B)\dot{y}, & y > -1, \\ Ky - 2A\dot{y}, & y \leqslant -1, \end{cases}$$

$$y = \frac{x}{d}, \quad \tau = \sqrt{\frac{k_1}{m}}t, \quad A = \frac{f_1}{2\sqrt{mk_1}}, \quad B = \frac{f_2}{2\sqrt{mk_1}}, \quad K = \frac{k_2}{k_1}, \quad F = \frac{F_0}{k_1 d} \quad \text{and} \quad \Omega = \omega\sqrt{\frac{m}{k_1}}.$$

In Eq. (3), the parameters A, B, K and F are assumed to be small and of order ε (>0).

Let $y = a\cos(\Omega\tau + \Phi)$, with $\Omega \approx 1$, be a solution of Eq. (3). Substituting this solution into Eq. (3) leads to

$$\begin{aligned} \frac{da}{d\tau} &= -\frac{1}{2\pi}\int_0^{2\pi} f(a\cos\Phi, -a\sin\Phi)\sin\Phi\, d\Phi - \frac{F}{1+\Omega}\cos\Phi, \\ \frac{d\Phi}{d\tau} &= 1 - \Omega - \frac{1}{2a\pi}\int_0^{2\pi} f(a\cos\Phi, -a\sin\Phi)\cos\Phi\, d\Phi + \frac{F}{1+\Omega}\sin\Phi. \end{aligned} \tag{4}$$

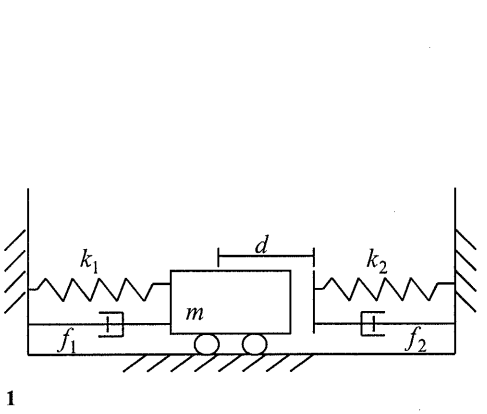

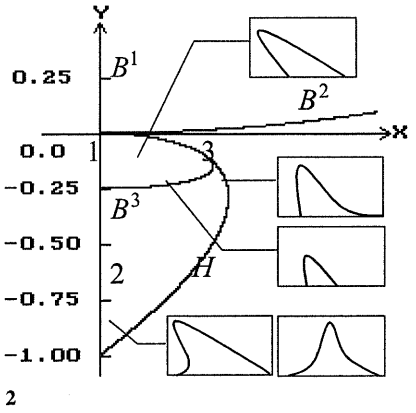

Fig. 1. Vibration system with piecewise-linearity.
Fig. 2. The transition set and the bifurcation diagram for $\sigma = 1.0$.

Integrating Eq. (4), the averaged equation for system (1) can be obtained as follows:

$$\begin{aligned}\frac{da}{d\tau} &= -\frac{1}{2\pi}[2a\pi(A+B) - 2aB\Phi_0 + aB\sin 2\Phi_0] - \frac{F}{1+\Omega}\cos\Phi,\\ \frac{d\Phi}{d\tau} &= 1-\Omega-\frac{1}{2a\pi}\left[Ka\left(\pi-\Phi_0-\frac{\sin\Phi_0}{2}\right)+2K\sin\Phi_0\right]+\frac{F}{a(1+\Omega)}\sin\Phi,\end{aligned} \tag{5}$$

where $\Phi_0 = \arccos(1/a)$.

Expanding Φ_0 and $\sin\Phi_0$ in terms of Taylor series, leads to

$$\Phi_0 = \arccos\frac{1}{a} = \frac{\pi}{2} - \frac{1}{a} - \frac{1}{6a^3} + O\left(\frac{1}{a^5}\right) \tag{6}$$

and

$$\sin\Phi_0 = 1 - \frac{1}{2a^2} + O\left(\frac{1}{a^4}\right). \tag{7}$$

Substituting (6) and (7) into Eq. (5), leads to

$$\begin{aligned}\frac{da}{d\tau} &= -\frac{2B}{\pi} - \frac{2A+B}{2}a + \frac{2B}{3\pi a^2} - \frac{F}{1+\Omega}\cos\Phi,\\ \frac{d\Phi}{d\tau} &= 1-\Omega+\frac{K}{4}+\frac{K}{a\pi}-\frac{K}{6\pi a^3}+\frac{F}{a(1+\Omega)}\sin\Phi.\end{aligned} \tag{8}$$

3.2. Local bifurcations for the steady states

By letting the right-hand side of Eq. (8) be 0, the frequency response of the system is given by the following equation:

$$\left[\left(\frac{2A+B}{2}+\frac{2B}{\pi}-\frac{2B}{3\pi a^2}\right)^2+\left(1-\Omega+\frac{K}{4}+\frac{K}{a\pi}-\frac{K}{6\pi a^3}\right)^2\right]a^3 = \left(\frac{F}{1+\Omega}\right)^2. \tag{9}$$

The local bifurcation of the steady state can be investigated by unfolding the steady state.

Writing

$$z=\frac{1}{a},\quad \alpha=\frac{B}{\pi},\quad \beta=\frac{K}{2\pi}\quad\text{and}\quad \gamma=\frac{F}{4},$$

the bifurcation equation is given by

$$G(z,\eta,\alpha_1,\alpha_2)=\left[\left(z-\frac{z^3}{6}\right)+\eta\right]^2+\alpha_1^2-\rho\alpha_1^2 z+\alpha_2 z^3, \tag{10}$$

where

$$\eta=\frac{1}{4}\left[\frac{1-\Omega^2}{\beta}+\pi\right],\quad \alpha_1=\frac{(1+\sigma)\pi}{4}\frac{\alpha}{\beta},\quad \alpha_2=\left(\frac{\rho}{2}\alpha_1\right)^2-\left(\frac{\gamma}{\beta}\right)^2,\quad \rho=\frac{8}{(1+\sigma)\pi}\quad\text{and}\quad \sigma=\frac{2A}{B}.$$

It can be shown that $G(z,\eta,\alpha_1,\alpha_2)$ is a two-parameter, α_1 and α_2, unfolding of the germ $g=[(z-\frac{1}{6}z^3)+\eta]^2$ (see [16]). From the physical point of view, α_1 represents damping and α_2 represents external force.

The transition set of G is

$$\sum = B\cup H\cup D,\qquad B=B^1\cup B^2\cup B^3, \tag{11}$$

where:

(a) the bifurcation point set is

$$B^1=\{\alpha_1=0\},\quad B^2=\left\{\alpha_2=\frac{\rho^2}{4}\alpha_1^2\right\},\quad B^3=\left\{\alpha_2=\frac{-(1-4\rho\alpha^2)\pm\sqrt{1-16\alpha^2+8\rho\alpha^2}}{8}\right\},$$

(b) the hysteresis set is

$$H=\left\{\alpha_1=\pm\sqrt{\frac{\alpha_2 z^4+[\alpha_2+(1-\frac{1}{2}z^2)^2]^2}{(\rho z-1)z^2}},\ \alpha_2=\frac{-c_2\pm\sqrt{c_2^2-4c_1c_3}}{8}\right\},$$

where

$$c_1=\frac{\rho}{z^2},$$
$$c_2=\frac{(1-\rho z)(2-z^2)}{z}+\rho z^2+\frac{\rho(2-z^2)^2}{2z^2}+2z(1-\rho z),$$
$$c_3=\frac{2(1-\rho z)}{z}\left(-1+\frac{1}{2}z^2\right)^3+\frac{\rho}{z^2}\left(-1+\frac{1}{2}z^2\right)^4,$$

(c) the double limit point set is $D=\emptyset$ (empty).

The transition set Σ of G divides the parameter plane, α_1–α_2 plane, into several regions, in each of which the diagrams of G are persistent, otherwise inpersistent on the transition set Σ. The transition set and the bifurcation diagrams are shown in Fig. 2 for $\sigma=1.0$, and Fig. 3 shows the transition set for $\sigma=10.0$.

From the physical point of view, only the persistent diagrams in regions 1, 2 and 3 and the inpersistent diagrams on H and B^3 are valid when $\sigma=1.0$. From Fig. 3, it can be seen that the jumping and the hysteresis phenomena appear in regions 2 and 3.

3.3. Stability of the steady states

As shown in Fig. 2, the jumping and the hysteresitic phenomena, see for instance [1], appear in region 2 with multiple solutions of the system. In order to see clearly, an amplified diagram of Fig. 2 is shown in Fig. 4. It can be shown that the points P_1, P_2 and P_3 in Fig. 4 are stable, unstable and stable steady states

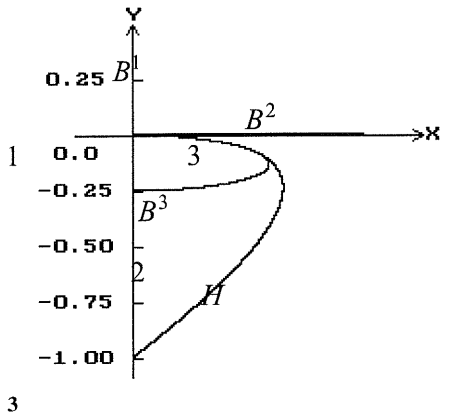

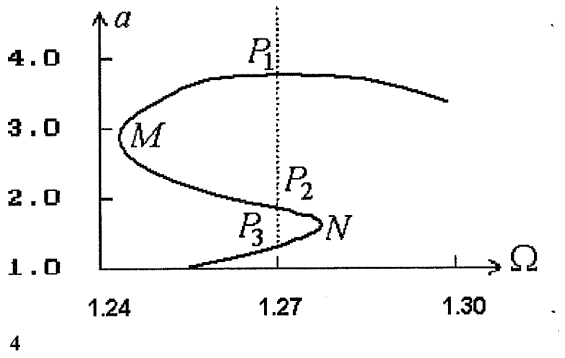

Fig. 3. The transition set for $\sigma = 10.0$.
Fig. 4. Multiple steady-state solution.

when $\Omega = 1.27$ and the amplitudes: 3.6486, 1.5665 and 1.1070, respectively. It can also be shown that the points M and N are the turning points with vertical tangent line.

Next, the stability of the multiple solution points P_1, P_2 and P_3 and the turning points M and N are studied.

Introducing the transformation

$$\begin{aligned} &x_1^2 + x_2^2 = a^2, \\ &\Phi = \operatorname{arctg}\left(\frac{x_1}{x_2}\right) \end{aligned} \tag{12}$$

into Eq. (9), the following equations can be obtained:

$$\begin{aligned} \dot{x}_1 &= -\left(\frac{2A+B}{2} + \frac{2B}{3a^2\pi}\right)x_1 + \frac{F\sin\Phi}{1+\Omega}x_2, \\ \dot{x}_2 &= -\left(\frac{K}{a^2\pi} - \frac{K}{2a^4\pi} + \frac{F\sin\Phi}{a^2(1+\Omega)}\right)x_1 + \frac{F\cos\Phi}{1+\Omega}x_2. \end{aligned} \tag{13}$$

The characteristic equation of (13) is $\lambda^2 + P\lambda + Q = 0$ with the discriminant $\Delta = P^2 - 4Q$, where

$$\begin{aligned} P &= 2A + B + \frac{2B}{a\pi} + \frac{B}{3a^3\pi} > 0, \\ Q &= \left(\frac{2A+B}{2}\right)^2 + \frac{B(2A+B)}{a\pi} + \frac{B(2A+B)}{6a^3\pi} + \frac{4B^2}{3a^2\pi^2} - \frac{4B^2}{18a^6\pi^2} \\ &\quad + \left(1 - \Omega + \frac{K}{4}\right)^2 + \frac{(1-\Omega+\frac{1}{4}K)}{a\pi} + \frac{(1-\Omega+\frac{1}{4}K)}{6a^3\pi} + \frac{K^2}{3a^2\pi^2} - \frac{K^2}{18a^6\pi^2}. \end{aligned}$$

It can be shown that M and N are two separatrix points between the stable and unstable solutions. Both M and N are saddle-node bifurcation points. In the same way, it can be shown that the points P_1, P_2 and P_3 are a stable node, a saddle point and a stable spiral-point, respectively, for the averaged Eq. (8).

The phase diagram of Eq. (8) is given in Fig. 5 showing the co-existence of the three solutions. In Fig. 5, W_1^u and W_2^u are the unstable manifolds of the saddle point P_2, and W_1^s and W_2^s are unstable manifolds of the saddle point P_2 which divide the phase plane into two regions, each of which is attracted by the stable points P_1 and P_3.

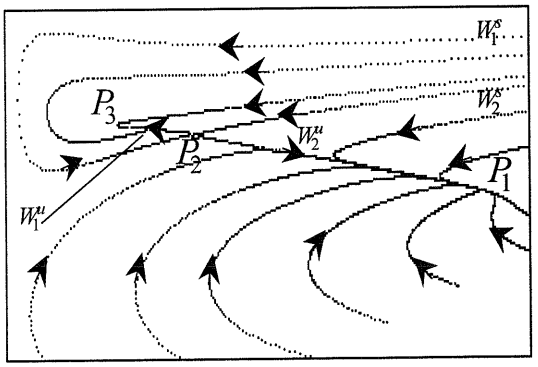

Fig. 5. Multiple solutions of the averaged system.

4. Period-doubling and chaos

In this section, the parameter k_1 is taken as the bifurcation parameter. The other parameters are taken as $m = 400$, $F_0 = 7.8 \times 10^3$, $\omega = 34.56$, $d = 5 \times 10^{-3}$, $f_1 = 50$, $f_2 = 500$ and $k_2 = 9 \times 10^5$.

By letting $\dot{x} = y$ in Eq. (3), the following system can be obtained:

$$\begin{aligned} &\dot{x} = y, \\ &\dot{y} = [-Q(x) - F(x,y) - F_0 \sin \omega t]/m, \quad (x,y,\theta) \in R^2 \times S, \\ &\dot{\theta} = 1, \quad (\theta \bmod 2\pi/\omega). \end{aligned} \tag{14}$$

Section $\Sigma = \{(x,y,\theta) \,|\, \theta = 0\}$ is taken to establish Poincaré map: $\Sigma \to \Sigma$.

Next, a fourth-order Runge–Kutta method and Poincaré section are used to find the periodic points, bifurcation phenomena and the phase portrait. The largest Lyapunov exponent of the system is used to detect chaos.

From Figs. 6–8, it can be seen that periodic solutions are obtained when $k_1 = 30.0 \times 10^3$, period-2 solution (1×2-cycle) when $k_1 = 20.0 \times 10^3$, and period-4 solution (2×2-cycle) when 5.0×10^3, respectively.

Period-doubling for 2×2-cycle, 4×2-cycle, 8×2-cycle and 16×2-cycle are shown in Figs. 9–12 when $k_1 = 2.0 \times 10^3$, 1.0×10^3, 0.7×10^3 and 0.697×10^3, respectively. The areas (rectangular boxes) shown in Fig. 12 are the local amplification near the period points.

In the same way, period-doubling can occur from period-3 solutions for certain value of the parameter k_1. The period-3 solution is shown in Fig. 13 when $k_1 = 4.0 \times 10^3$; 3×2-cycle and 6×2-cycle are shown in Figs. 14 and 15 when $k_1 = 2.0 \times 10^3$ and 1.5×10^3, respectively.

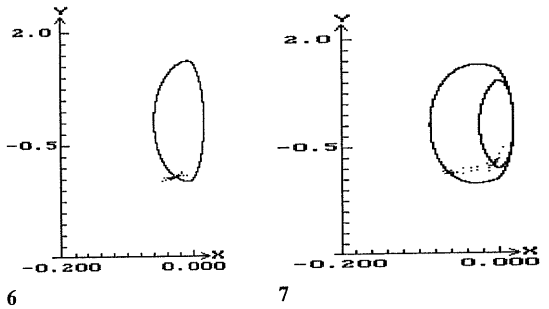

Fig. 6. Period-1 solution.

Fig. 7. Period-2 solution.

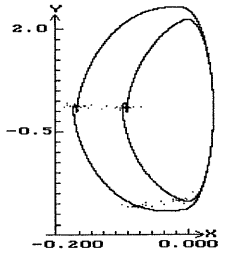

Fig. 8. Period-4 solution.

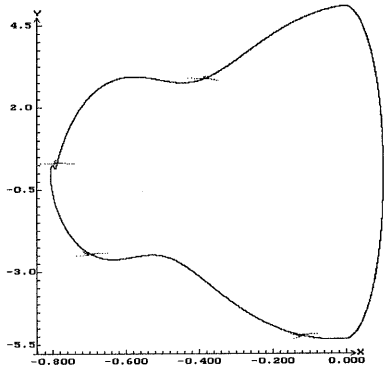

Fig. 9. Period-4 solution.

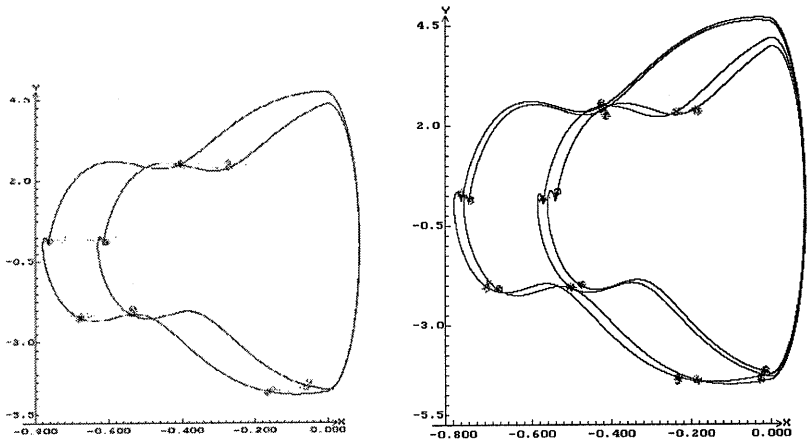

10 11

Fig. 10. Period-8 solution.
Fig. 11. Period-16 solution.

From the above figures, it can be seen that system (1) exhibits period-doubling, period-3 bifurcation and then chaos. It can also be verified that $k_1 = 4.0 \times 10^3$ is the threshold to chaos.

It is worth noticing that both period-4 and -6 attractors (Figs. 9 and 14) obtained when $k_1 = 2.0 \times 10^3$ for the system with piecewise-linearity, depend on the initial conditions taken. In other words, the

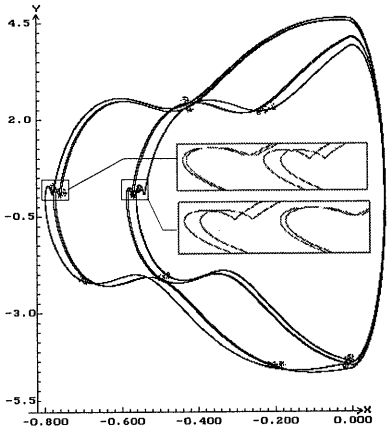

Fig. 12. Period-32 solution.

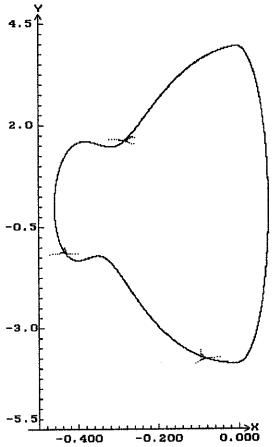

Fig. 13. Period-3 solution.

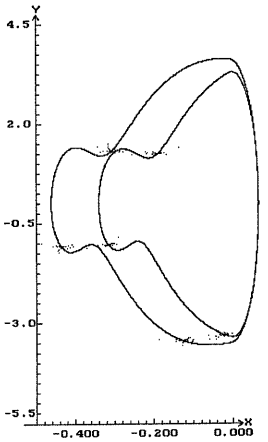

Fig. 14. Period-6 solution.

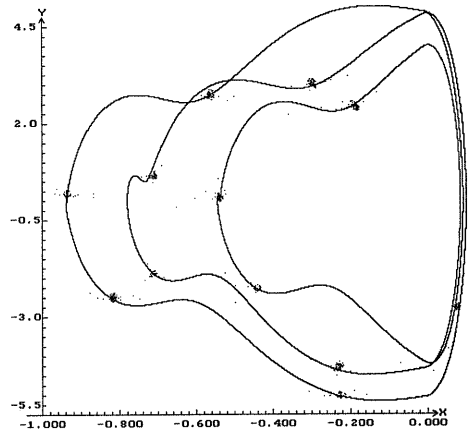

Fig. 15. Period-12 solution.

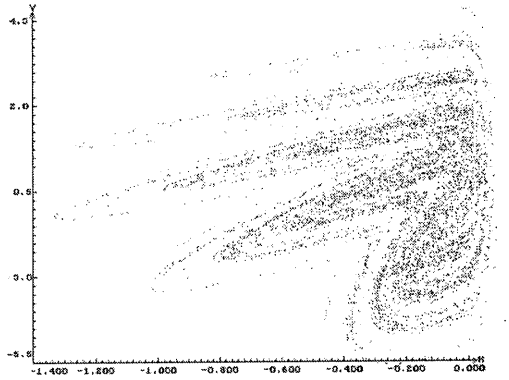

Fig. 16. Chaotic motion of the piecewise-linearity vibration system.

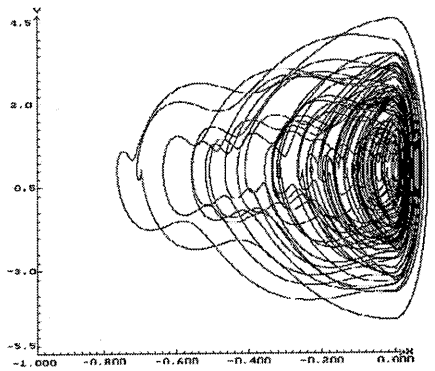

Fig. 17. Phase portait of the piecewise-linearity vibration system.

co-existence of different attractors can be found in the same system for the same values of the parameters. The attracting field of each attractor can be determined by means of cell-map.

Figs. 16 and 17 show the chaotic attractor and the phase portrait for $k_1 = 0.1 \times 10^3$.

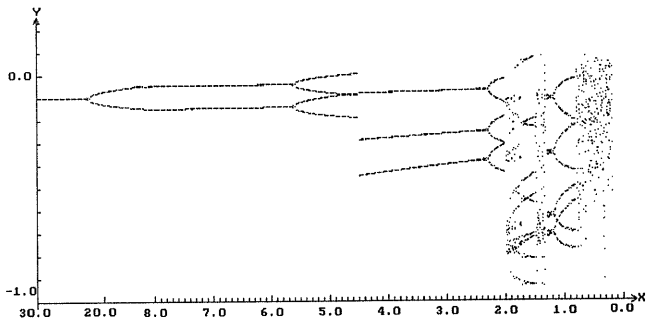

Fig. 18. Period-doubling and period-3 bifurcation to chaos for the piecewise-linearity vibration system.

Fig. 18 shows the bifurcation diagram for k_1 over [30,0]. From this figure, it can be seen that the system exhibits period-doubling, period-3 solution and then chaos.

5. Conclusion

In this paper, bifurcation behaviour for a class of vibration system with piecewise-linearity has been studied numerically. Local bifurcation and the stability of the steady-state solutions of the system have been studied using C–L method (which is used to obtain the averaged system of the oscillator). Poincaré map was introduced to find periodic solutions, period-doubling and period-3 bifurcations. The route to chaos from period-doubling bifurcation has been investigated by examining the phase plane, bifurcation diagram and the largest Lyapunov exponent. From the results obtained, it is found that the piecewise linear system exhibits complex dynamical behaviour.

Acknowledgements

Qingjie Cao gratefully acknowledges of the support of the National Science Foundation of China, State Scholarship Council of China and the Natural Science Foundation of Shandong Province, China.

References

[1] Chen YS, Andrew YLL. Bifurcations and chaos in engineering. London: Springer; 1998.
[2] Lorenz E. Deterministic nonperiodic flow. J Atmos Sci 1963;2:130–41.
[3] Awrejcewicz J, Bajaj AK, Lamarque CH. Non-linearity, bifurcation and chaos: the doors to the future. Int J Bifurc Chaos 1999;9(2):305–6.
[4] Kapitaniak T, Bishop SR. The illustrated dictionary of nonlinear dynamics and chaos. Chichester: Wiley; 1999.
[5] Komatsu Y, Kotani S, Matsumura A. A period-doubling bifurcation for the Duffing equation. Osaka J Math 1997;34(3):605–27.
[6] Li TY, York JA. Period three implies chaos. Am Math Monthly 1975;82:985–90.
[7] Sharkovsky AN. Coexistence of cycles of a continuous map of a line into itself. J Ukrain Math 1964;16:61–71.
[8] Devaney RL. Introduction to chaotic dynamical systems. New York: Benjamin; 1989.
[9] Freire E, Ponce E, Rodrigo F, Torres F. Bifurcation sets of continuous piecewise linear systems with two zones. Int J Bifurc Chaos 1998;8(11):2073–97.
[10] Aziz-Alaoui MA. Differential equations with multispiral attractors. Int J Bifurc Chaos 1999;9(6):1009–39.
[11] Lu LY, Song QG, Wang XX, Huang MG. Analysis of bifurcation and chaos of tension-slack oscillator by Lyapunov exponent. Mech Res Commun 1997;24(5):537–43.
[12] Raghothama A, Narayanan S. Bifurcation and chaos in geared rotor bearing system by incremental harmonic balance method. IEICE Trans Fund Electron Commun Comput Sci 1997;E80A(9):1567–71.
[13] Kohari K, Saito T, Kawakami H. Chaos and fundamental bifurcation phenomena from a relaxation oscillator with periodic thresholds. Electron Commun Jpn III 1995;78(7):79–88.
[14] Ohnishi M, Inaba N. A singular bifurcation into instant chaos in a piecewise-linear. IEEE Trans Circuits Syst I 1994;41(6):433–42.

[15] Jinno K. Chaos and related bifurcation phenomena from a simple hysteresis network. IEICE Trans Fund Commun Comput Sci 1996;E79A(3):402–14.
[16] Freire E, Ponce E, Ros J. Limit cycle bifurcation from center in symmetric piecewise-linear systems. Int J Bifurc Chaos 1999;9 (5):895–907.
[17] Guckenheimer J, Holmes P. Nonlinear oscillation dynamical systems and bifurcations of vector fields. New York: Springer; 1983.